Construction and Building Materials 299 (2021) 123854

Contents lists available at ScienceDirect

Construction and Building Materials

journal homepage: www.elsevier.com/locate/conbuildmat

Evaluating the performance of sonic and ultrasonic tests for the inspection of rammed earth constructions

J.D. Rodríguez-Mariscal [a], J. Canivell [b], M. Solís [a,*]

[a] Escuela Técnica Superior de Ingeniería, Universidad de Sevilla, Camino de los Descubrimientos, Sevilla 41092, Spain
[b] Department of Architectural Construction II, Universidad de Sevilla, Av. Reina Mercedes 4, Sevilla 41012, Spain

HIGHLIGHTS

- Wave propagation velocities are measured on medium size specimens.
- An automated procedure is presented for the identification of the time-of-flight.
- Results are obtained for different damage levels after compression loads are applied.
- Results illustrate the sensitivity to loading history and specimen heterogeneity.
- Sonic tests are more stable, reliable and sensitive than ultrasonic tests.

ARTICLE INFO

Article history:
Received 22 February 2021
Received in revised form 31 May 2021
Accepted 1 June 2021

Keywords:
Rammed earth
Non-destructive tests
Sonic test
Ultrasonic test
Compaction energy control

ABSTRACT

There are many examples of historical rammed earth constructions for which the development of valid methods for evaluation of their conservation state is a major concern for conservation agencies of all around the world. On the other hand, rammed earth is attracting the attention of modern architecture trends because of its outstanding performance from an ecological perspective. Thus, the development of reliable non-destructive tests for the inspection of new and existing rammed constructions is of major interest. Ultrasonic and sonic tests are among the most commonly used. While the former has been the subject of numerous studies in rammed earth soil, sonic tests still requires further experimental development. In general, both tests demand a more precise study of their performance according to different states of loading and damage to evaluate the state of structural degradation. Additionally, the procedure commonly used to apply both tests need to be revised in order to provide a more reliable and precise assessment of the time-of-flight of elastic waves. Therefore, on the one hand, this paper evaluates and compares the sensitivity of both non-destructive inspection techniques to different levels of damage induced on the tested samples and possible heterogeneous properties such as compaction energy distribution during the manufacturing process. On the other hand, an automated procedure for the analysis of the experimental recordings and the identification of the time-of-flight of sonic and ultrasonic waves is developed to facilitate the applicability of these techniques. This new procedure consists of a simple signal analysis algorithm that avoids the time-consuming task of manual inspection of the signals and reduces uncertainty in the final results. The results show that sonic test is a valid a promising tool for the inspection of this type of constructions. It performs better than ultrasonic test, which could also be used in practice with some limitations.

1. Introduction

The use of earth as a building material is a common practice all around the world since ancient times. Earth constructions exhibit attractive features that have been observed by many authors, such as good insulation (thermal and acoustic), fire resistance, low cost, easy to handle, etc [1]. In modern architecture, there is a revival of the use of earth because of its excellent performance from an environmental perspective: low emissions, no demolition waste, possible use of industrial by-products or recycled aggregates as additives, etc. Relevant architectural projects committed with environmental preservation use earth as a modern building material. Significant examples of these projects can be found in the

* Corresponding author.
E-mail address: msolis@us.es (M. Solís).

https://doi.org/10.1016/j.conbuildmat.2021.123854
0950-0618/

Terra Award competition (http://terra-award.org/). However, there is still a lack of guidelines and standards for the structural design, quality control, inspection, etc [2–6].

Rammed earth is one of the traditional techniques that use soil as a building material. It is the most common technique in earthen heritage sites in Spain [7]. It mainly consists in pouring and compacting a certain amount of moist soil (called layer) into a mold. The thickness of a layer is usually between 100 m and 150 mm. Rammed earth walls are built up by adding successive layers. Traditionally, the compaction process is performed manually by using wooden rammers. Nowadays, electro-mechanic and pneumatic compaction hammers are usually considered in modern architectural projects.

Apart from the advantages mentioned previously, rammed earth has other virtues derived from its construction technique. For example, by using a small amount of water for mixing, it is quick to execute and improves the production output of the construction site. However, aspects such as high thermal conductivity are disadvantages, especially in terms of compliance with certain building regulations. In this respect, several authors have proposed external improvements such as coatings [8] or the use of various additives to reduce thermal conductivity without compromising mechanical properties [9].

As for other types of construction techniques, various instrumental techniques for the physico-mechanical characterisation of rammed earth are being studied and developed. These are indispensable both for the control of the execution and for the inspection of existing structures. So far, some pioneering recent works have been published about the use of slightly destructive or non-destructive techniques. Related to the first, Lombillo et al. [10] applied the flat-jack, hole-drilling and mini-pressuremeter techniques to in situ evaluate the stiffness and deformation. In [11,12], the rebound index technique was used, and different compaction levels could be detected within different layers of rammed earth specimens. This phenomenon can be more significant for higher layer thickness. A homogenization approach can be used to account for this issue in the numerical modeling of rammed earth layers [13].

Non-destructive techniques based on the propagation of elastic waves are well known and have been successfully applied for the inspection of building materials. They are based on the fact that the wave propagation velocities (WPV) depends on the density and the stiffness of the material (Young modulus and Poisson coefficient for linear elastic isotropic materials). Moreover, the wave propagation can be affected by the presence of damage (cracking, voids, etc.). The WPV is determined by measuring the time that an elastic wave takes to travel from one point to another located at the boundary of the solid. An emission probe is located at one point and excites the solid (usually with an excitation pulse), whereas a receiver probe detects the arrival of the wave at a different point. An accurate and precise measure of this time is a major challenge when applying these techniques. Depending on the frequency content of the excitation, the WPV can be determined in the sonic range or ultrasonic range. Thus, the Sonic Wave Propagation Velocity (SWPV) or the Ultrasonic Wave Propagation Velocity (UWPV) can be identified.

Studies on UWPV applied on compacted soil have been addressed by several authors, who in general demonstrate the possibilities and limitations of this approach for the indirect characterisation of this material. An empirical analysis of the relationship of some physical–mechanical properties of lime-stabilized rammed earth (dry density, effective porosity, moisture content and compressive strength) with UWPV has been studied by Canivell et al. [14]. They found that UWPV can be a promising tool for quality control of rammed earth samples. Those with higher density and lower porosity exhibited higher UWPV. A relationship between UWPV and moisture content (MC) or compressive strength was not found in that work. However, the presented results showed that higher UPWV is likely to be found for higher compressive strength samples. In a later work [15], the same authors found some direct relationship between compressive strength and UWPV perpendicular to the compaction direction, whereas an inverse relationship was found for the UWPV in the compaction direction.

However, there are some factors that may influence the UWPV measurements [16] and also the mechanical properties, such as the moisture content and the hygrometric equilibrium process. As with any natural building material, the MC and the process of hygrometric equilibrium can affect the mechanical properties of rammed earth [17]. The influence of the MC during the curing process of rammed earth samples on UWPV was analyzed in [18]. It was found that UWPV increased as the water content decreased during the drying process until the hygrometric equilibrium took place.

The UWPV and SWPV techniques can serve as tools for the control of the execution of new building structures and for the inspection of existing ones, which is especially valuable for the conservation of cultural heritage sites. In that sense, a UWPV tomography of ancient unfired earth bricks of an archaeological site was applied by Aguilar et al. [19]. They found that the UWPV could be used to classify bricks from different soil types and also to detect damaged bricks.

The sonic tests are not so well-known and established as the ultrasonic tests for the inspection of materials and structures. It has been tested and developed for the last two decades (see for instance [20,21]). In the case of rammed earth, SWPV have been proved to be sensitive to damage and grout injection in repaired wallets [22,23]. Silva et al. [24] determined the SWPV of new rammed earth walls perpendicular to the compaction direction. They found similar values than those previously obtained in [25] for a historic building.

In order to apply these non-destructive inspection techniques whether for the analysis of the state of conservation or quality control in execution of rammed earth constructions, it is still necessary prior scientific studies that analyze their sensitivity to damage and variation of construction parameters. The use of these techniques to quantify the presence of voids, cracks, defects, etc, is a very valuable and established approach for many engineering materials. However, it is yet a research challenge to be addressed for rammed earth in practice. This paper is aimed at carrying out a first step in that direction by evaluating the effect of the applied load on rammed earth specimens and evaluate the sensitivity of the ultrasonic and sonic tests to induced global damage. It contributes to the development of the required prior knowledge by evaluating and comparing the performance of sonic and ultrasonic tests in order to shed light on which technique is more suitable for certain conditions. To that end, six medium size specimens were manufactured. A grid of measuring points is defined for each specimen, so the gradients of WPV are analyzed in order to study the capability of the non-destructive tests to identify possible heterogeneous properties of each specimen. In addition, the UWPV and SWPV are determined after different compressive loads were applied, so the effect of cumulative damage on WPV is analyzed.

For the practical development of these techniques, it is also necessary to develop simple and useful tools that simplify the traditional time consuming and subjective task of visual inspection of the recorded signals to identify the time of arrival of the elastic waves. For the ultrasound inspection, some black-box software applications provided by the manufacturers are usually available to automatically estimate the UWPV. However, for the sonic tests, no commercial software is available. In addition, the analysis of the raw signals is a more rigorous approach for scientific applications, specially at preliminary stages. For this purpose, the other

objective of this paper is to present an automated procedure, that can be easily controlled and adapted by the user, for WPV identification. It is based on some simple criteria to define the time the pulse excitation begins and the time the elastic wave arrives to the receiver. The criteria are based on a set of parameters and the optimal set is selected by an automated search.

The outline of the paper is as follows. First, the physical-mechanical properties and manufacturing process of the specimens are presented. The specimens were manufactured under controlled conditions in order to reduce the influence that different values of MC and compaction energy could have on the identified WPV. The paper presents a simple method to accurately control the compaction energy of each layer. Next, the compression and non-destructive tests are described. The details about the algorithm for the automated analysis of time recording signals are presented. The values of the UWPV and SWPV for each measuring point and for three different load levels are presented and discussed in the next section. Finally, conclusions are drawn and some future works are outlined in the last section.

2. Materials and methods

Six specimens (named from V1 to V6) were manufactured and tested. Their dimensions were [300x300x600]mm^3 (Fig. 1(a)). A description of the physical properties of the soil, manufacturing process and destructive and non-destructive tests is provided next.
.

2.1. Soil properties

The particle size distribution affects the voids ratio and contact between grains of the material. In this work, the sub-soil was selected and analyzed by a local organization experienced in earth construction within the framework of Eramus + Project 'LearnBION – Learn Building Impact Zero Network'. The soil was selected for the construction of a new small building in Valverde de Burguillos (Spain).

The particle size distribution of the selected sub-soil was determined according to Spanish Standard [26]. Fig. 2 shows the obtained result. When compared with the well-known Fuller curve as a reference, a good agreement is found for the sand fraction, but the selected sub-soil exhibits a slightly excessive portion of gravel and lack of silt and clay. The soil can classified as fine to coarse sand (SW), according to the Unified Soil Classification System.

The Liquid Limit and Plastic Limit of the soil were determined by following Standard procedures [27,28]. The obtained values were 30.3% and 18.0%, respectively.

2.2. Compaction process

The compaction process is a critical issue for quality control in rammed earth construction, as it rearranges the particles, decreases the porosity index and subsequently increases the dry density. A higher compaction theoretically increases the stiffness and mechanical strength of the soil. Traditionally, the earth is poured into the mold and manually compacted until a 'ringing' sound is noticed. This sound indicates that the compacted soil is exhibiting 'high' stiffness. However, this is a very qualitative criterion that depends very much on the person in charge of the process. Moreover, once the 'ringing' sound is achieved, it does not significantly change even though the compaction process continues. Thus, this subjective criterion can be used in practice to ensure a certain level of compaction but not as a measure of the actual compaction energy that has been applied. This energy depends on the weight of the rammer, the drop height, and also depends

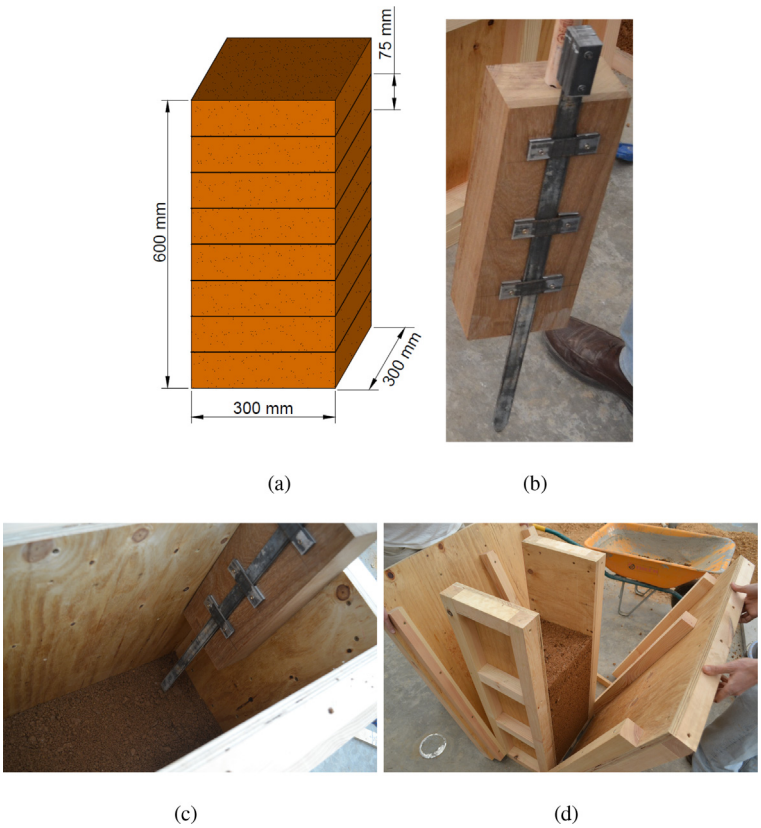

Fig. 1. (a) Scheme of the specimens. (b) Detail of the designed rammer for controlling the compaction energy. (c) Rammer inside the mold. (d) Removal of the mold.

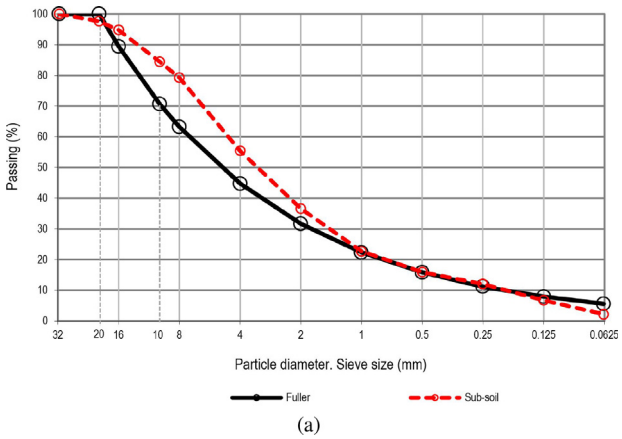

Fig. 2. Particle size distribution of the selected sub-soil.

on the force applied by the mason by pushing the rammer against the earth when being dropped. There are some previously published works that study the effect of different compaction methods (static or dynamic) on the OMC, maximum dry density and compressive strength [29–31]. However, to the author's knowledge, the measurement and control of the manual compaction process in practice, including the actually applied compaction energy and its effect on the mechanical performance of rammed earth have not been thoroughly addressed in the literature yet.

In this work, manual compaction has been tackled using a traditional wooden rammer, and the compaction energy was controlled by counting the applied impacts and the drop height. The latter was controlled by means of a steel guide attached to the rammer (Fig. 1 (b) and (c)). The tip of the steel guide lays on the top surface of the specimen under construction, and the rammer can slide along the guide. A block of metal is attached to the guide and serves as an upper limit for the movement of the rammer. By fixing the block at the desired position, the drop height of the rammer is easily controlled. The rammer is just dropped to let it impact the soil, without applying any extra force that could not be otherwise measured.

In order to obtain a compaction level in agreement with usual practical values applied in real constructions, the number of impacts and drop height was defined following the recommendations of a local experienced mason in rammed earth construction. The weight of rammer was 6 kg, the drop height was 300 mm and the number of impacts per layer was 65. The initial thickness of each layer when poured into the mold was 110 mm, and its final thickness was 75 mm. Considering that the area of the specimen was [300x300]mm^2, the applied compaction energy was 364 kJ/m^3. After six layers were poured and compacted, the wooden mold was removed and the specimen was dried in laboratory conditions (Fig. 1 (d)).

2.3. Moisture content

The effect of the MC on the mechanical behavior of rammed earth has been partially addressed in the literature [18,32]. Because of the presence of gravel, the MC of rammed earth is typically lower than other earthen construction techniques such as cob or adobe. However, unfortunately, there is not a rigorous standard criterion to define the Optimum Moisture Content (OMC) for any of them.

The Standard Proctor Test [33,34] and the Modified Proctor Test [35,36] are well-known standards for the determination of the OMC of the soil in civil and geotechnical engineering. The OMC is obtained for a controlled compaction energy of 583 kJ/m^3 and 2700 kJ/m^3. respectively, following a specific manufacturing process of specimens of specific dimensions from samples of soil sieved to a maximum particle size of 20 mm. However, the OMC of a soil increases as the compaction energy is smaller (and vice versa) so, consequently, the OMC should be ideally determined considering the compaction energy that is actually applied during construction. Moreover, the characteristics of the compaction process (manual, pneumatic or mechanical, size of the rammer, size of the wall or specimen, etc.) and the existence of bigger particle size fractions can also affect the final dry density and the OMC. Thus, the OMC obtained from a Standard or Modified Proctor Test should be considered with caution when applied for rammed earth construction. However, due to the lack of a specific standard method, the Proctor test has been used as a reference value in previous rammed earth research works (Table 1). By following the same reference criterion, the OMC obtained from a Standard Proctor Test for the selected soil in the present work (5.1%, Fig. 3) was considered as the target value during the manufacturing process, even though the applied compaction energy on the manufactured specimens was smaller than that of the Standard Proctor Test. It must also be noted that the obtained OMC is lower than usual values for rammed earth. This result can be explained by the relative high portion of gravel and low portion of silt and clay, as illustrated in [37,38]. As the proportion of gravel increases, the OMC is expected to decrease, since the specific surface area of the soil grains decrease.

In order to obtain the desired MC during the manufacturing process, the initial MC of the soil was previously determined by oven drying samples of the soil for 24 h, according to Spanish Standards [42]. This test was repeated for three samples during five days before the specimens manufacturing. Previously, the soil had been left to dry for one week in laboratory conditions so that it could reach a hygroscopic equilibrium before the determination of its MC. An initial MC of 1.03% was measured, so the required additional water to be added to the soil could be determined.

The soil and the added water were mixed in a concrete mixer. One mixture was made per each of the manufactured specimens. The final moisture of each specimen was determined by oven drying three samples per specimen following the same procedure as for the initial moisture [42]. Table 2 shows the moisture of each specimen, except for specimen V6, for which no value was measured. It can be observed that values are close but generally slightly lower than the target value. This can be due to some evaporation [43] or some water retention in the concrete mixer.

The mechanical behavior of rammed earth at any time can be affected not only by the MC during the manufacturing process but also by its MC at any time. The manufactured specimens were stored during approximately 90 days in the laboratory before they were tested. The length of this period was established according to the organization of the activity at the laboratory, considering that strength and other physical parameters are expected to be stable after 28 days approximately after manufacturing. Moreover, it is assumed that the longer the curing period is, the more stability

Table 1
OMC obtained for rammed earth specimens in previous works.

OMC [%]	Method	Reference
7	Standard Proctor	[12]
18.5	Standard Proctor	[14]
11.19	Standard Proctor	[15]
15	Standard Proctor	[17]
10.1–10.2	Standard Proctor	[24]
12,13.1–15.6	Modified Proctor	[39]
7–9	BS 1377 – Part 4	[40]
9–10	–	[41]

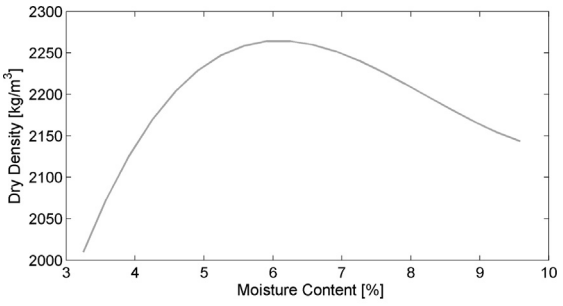

(a)

Fig. 3. Resulting curve from Standard Proctor test for the determination of the OMC.

is achieved. During this period, the average environmental conditions were 24.0°C (2°C standard deviation) temperature and 65.5% (4.8% standard deviation) relative humidity. Just after the compression test of each specimen, its MC was determined following Spanish Standards [42] from three samples of the specimen that included material from its inner and outer parts. The obtained values are shown in Table 2. Except for specimen V1, the values are very similar for all the specimens.

2.4. Dry density

Dry density is closely related to porosity, as both take into account the amount of voids (volume of air) contained in a specific mass. In fact, both physical parameters can be determined by the same test procedure [44]. Thus, a certain correlation between density-porosity and mechanical strength can be expected. However, some uncertainties still exist, since other soil and manufacturing properties (particle size distribution, particles shapes, compaction process, MC, additives, etc.) can affect the final mechanical behavior of the rammed earth [40]. For instance, in [41], a range from 1700 to 2400 kg/m^3 was observed for samples with compression strength values between 1.5 and 4.0 MPa. However, values below 1 MPa (in the range between 0.67 and 0.97 MPa) were obtained for samples of dimensions [300x300x600]mm^3 and dry density between 1763 and 2027 kg/m^3.

The average dry density of the specimens (dry mass per unit volume) was 1927.7 kg/m^3. This value is lower than the maximum dry density obtained from the Proctor Test (2250 kg/m^3), probably due to a lower compaction energy, lower MC during manufacturing, different molds and the presence of a low portion of gravel of size bigger than 20 mm. Nevertheless, the obtained dry density is a medium value when compared with the usual range from 1700 kg/m^3 to 2200 kg/m^3 defined in [45].

2.5. Compression tests

After the curing process of the specimens detailed in Section 2.3, simple compression tests were carried out. A universal monoaxial servohydraulic testing frame was used. The tests were displacement controlled at 3 mm/min rate.

In order to address the analysis of the sensitivity of SWPV and UWPV to cumulative damage induced by applied compressive loads, two previous loading–unloading processes to increasing maximum load levels were carried out for each specimen. Therefore, the WPV could be determined after different load levels had been withstand by the specimens and the effect of cumulative damage on WPV could be subsequently analyzed. Finally, after the loading–unloading processes, a monotonically increasing load was applied until rupture and the compressive strength was determined.

The first unloading was established when a load of 36kN (equivalent to 0.4 MPa compressive stress) was reached. A second loading–unloading cycle was performed at a maximum load level of 72kN (0.8 MPa) for specimens V1, V2, V3, V6 and 50kN for specimens V4, V5 (0.55 MPa). A lower value was considered for V4 and V5 because it was considered that 0.8 MPa was too close to the compressive strength of the specimens once the specimens V1, V2, V3 and V6 had been tested. Indeed, the second loading–unloading process could not be performed for specimens V2 and V3 since they failed before the specified maximum load of the loading process was reached. The values of the compressive strength of each specimen are included in Table 2:

2.6. Non destructive tests

The velocity of propagation of volumetric type P elastic waves can be determined by introducing an excitation at one point on one side of the specimen and measuring the time (time-of-flight) that the elastic wave takes to reach the opposite side, where a sensor is attached to detect the arrival of the wave. This type of test is known as direct test. The velocity is obtained by dividing the distance between source and receiver and the time-of-flight. Depending on the type of the excitation (namely the frequency content) and the characteristics of the sensors, the test is called sonic or ultrasonic.

It must be noted that, in the presence of voids, cracks, defects, etc., the wave might not travel following a straight path between the source and the receiver. As a result, it must be bear in mind that the determined velocity is actually an 'apparent' velocity and not the real velocity value.

For the ultrasonic tests, a *Pundit Lab* system from Proceq company was used. Two 24 kHz piezoelectric sensors were used. Both can work either as the excitation or the receiver probe. The sensors of the lowest available frequency in the market were selected in order to inspect a distance as long as possible. A pulse of 500 V amplitude was established as the excitation signal. The equipment provides the signal of the receiver after the time the excitation pulse is generated. This signal is analyzed as explained in the next section to identify the time-of-flight of the elastic wave. A total of 10 excitation pulses were processed at each measuring point by following the identification procedure described in next section.

For the sonic tests, the excitation is performed by using a small impact hammer of 11 mV/N sensitivity with a hard tip (model 056C01 from PCB company). The response is measured by using piezoelectric accelerometers of 100 mV/g sensitivity (model 256HX-100 from Endevco company). The accelerometers were fixed to the surface of the specimens by attaching them to a light

Table 2
MC during manufacturing, MC during the compression test, compressive strength of each specimen and their mean value and standard deviation (std).

Specimen	V1	V2	V3	V4	V5	V6	mean	std.
MC Manufacturing Process [%]	5.029	5.34	4.85	4.81	5.13	–	5.032	0.216
MC Compression Test [%]	0.33	0.63	0.56	0.56	0.63	0.55	0.54	0.11
Compressive Strength [MPa]	1.0615	0.7678	0.7439	0.6375	0.7535	1.0331	0.8329	0.1726

mounting base previously glued to the specimen by using wax. The signals were processed using a LAN-XI dynamic analyzer module from Brüel and Kjaer. The maximum available sample frequency (65536 Hz) was used. A total of 30 impacts were applied and recorded independently at each measuring point. The time signals were also processed by following the identification procedure described in next section.

The wave propagation velocities were determined at 9 points distributed on two side faces of the specimen. These points are arranged into three groups according to their relative height, namely: lower (B1, B2, B3), middle (M1, M2, M3) and upper (T1, T2, T3). (Fig. 4). Thus, the waves travel perpendicular to the manufacturing compaction direction. The velocities are measured before each loading–unloading cycle during the compression tests. Their values are referred as corresponding to *Load 0* (no previous load applied), *Load 1* (after the cycle at 0.4 MPa maximum stress is applied) and *Load 2* (after the cycle at 0.8 MPa or 0.55 MPa maximum stress is applied).

2.7. Automated procedure for WPV identification

The most critical point for identifying the wave propagation velocities is the identification of the time that the sensors detect the movement induced by the elastic wave, from which the time-of-flight of the elastic wave is determined. The difficulty lies on the fact that the signals from the sensors are contaminated with background ambient noise. Thus, the quality and robustness of the identification procedure depends mainly on the signal-to-noise ratio of the sensor. This ratio depends on the sensor sensitivity, amplitude of the incident elastic wave (depending on the excitation amplitude and distance between source and receiver), ambient noise (electric and physical environmental noise), etc.

In the case of ultrasonic excitation, the excitation is controlled by the measuring equipment. Thus, the time the elastic wave is generated is accurately controlled and provided by the equipment. As a result, it is only necessary to analyze the signal of the receiver. In contrast, during the sonic tests, the excitation is manually induced with the impact hammer. In this case, the time the excitation begins has to be identified by analyzing the time history of the signal of the hammer.

Fig. 5 (a) shows an example of the time history of the impact hammer and the accelerometer of one sonic test. Apparently, the time-of-flight can be easily determined by visual inspection of the plot. However, its precise determination is significantly affected by the presence of noise, as it can be seen in Fig. 5 (b). Traditionally, the time-of-flight is determined by visual inspection of the signals without any standard criteria. As a result, the human factor plays an important role and the results can be very much affected by subjective perception, zoom level used for the analysis, etc. A clear illustration of the scattering of the results produced by different human approaches can be found in [46]. Besides the uncertainty in the results, the visual inspection approach makes a sonic test inspection very time consuming and might discourage from the application of this type of test in practice.

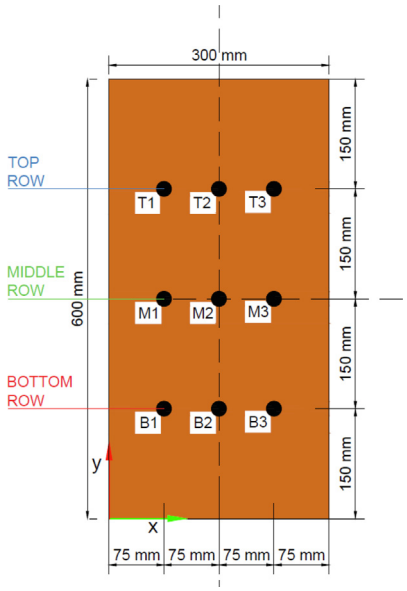

Fig. 4. Measuring points grid for non-destructive tests.

In this paper, an automated procedure for the determination of the time-of-flight is proposed. The authors are only aware of one previously automated approach published in the literature [47]. The methodology proposed in this paper is more robust since it considers a more complete set of criteria based on noise analysis, signal shapes and statistical variables. A set of conditions is defined in order to establish a criterion to identify the time the excitation starts and the wave arrives for the exciter and receiver sensors, respectively. These conditions are defined through a corresponding set of parameters, which are described as follows:

- The first step of the time-of-flight identification strategy is the characterization of the ambient noise of each signal. A sample recording of the ambient noise is obtained for each test from the time period before the sensor indicates the impact excitation (one second of pre-trigger recording was established for the sonic tests) or a time window before the arrival of the wave in the case of the receiver. The average value (μ_{noise}), which is usually close to zero, and the standard deviation (σ_{noise}) of the ambient noise recordings from these time periods are evaluated. The time the excitation impact starts or the elastic wave arrives can only be determined if the reading of the sensor is significantly higher than the amplitude of the ambient noise. Thus, the value of a candidate reading (s_i) has to be higher than the average value of the noise plus a number of times (parameter α) the standard deviation of the noise, as stated in Eq. (1). A different value of this parameter can be defined for the excitation (α_{exc}) and the receiver (α_{rec}).

$$|s_i| > |\mu_{noise} \pm \alpha \cdot \sigma_{noise}| \quad (1)$$

  - Once a sample that satisfies the previous condition has been found, it must be checked if the signal follows an increasing or decreasing trend due to the impact or wave arrival effect. Thus, a similar criterion is applied to subsequent readings (*NPt*) considering a higher deviation from the ambient noise through parameter β (β_{exc} for the excitation and β_{rec} for the receiver) as it is written in Eq. (2).

$$|s_{i+j}| > |\mu_{noise} \pm \alpha \cdot \beta \cdot \sigma_{noise}| \rightarrow \text{from } j = 1 \text{ to } j = NPt \quad (2)$$

  - Lastly, in order to ensure that the signal has certainly a significant progressively increasing or decreasing trend, the ratio of the values of the first and last sample for which the previous conditions have been fulfilled has to be greater than a certain value (parameter *NRatio* in Eq. (3)).

$$\frac{s_i}{s_{i+NPt}} > NRatio \quad (3)$$

The readings of each time signal are analyzed subsequently by progressively applying the previous conditions. The first sample that fulfills all the criteria is selected. Then, once the time of the start of the excitation and the arrival of the elastic wave are identified, the time-of-flight is determined and the WPV evaluated. A total of 10 pulses and 30 impacts were recorded for the

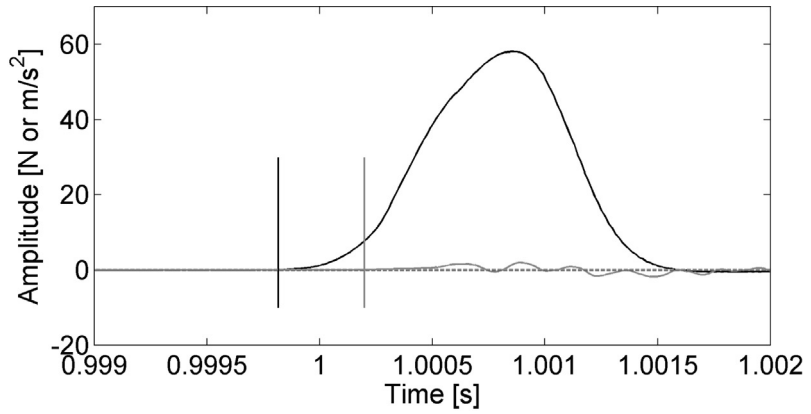

(a)

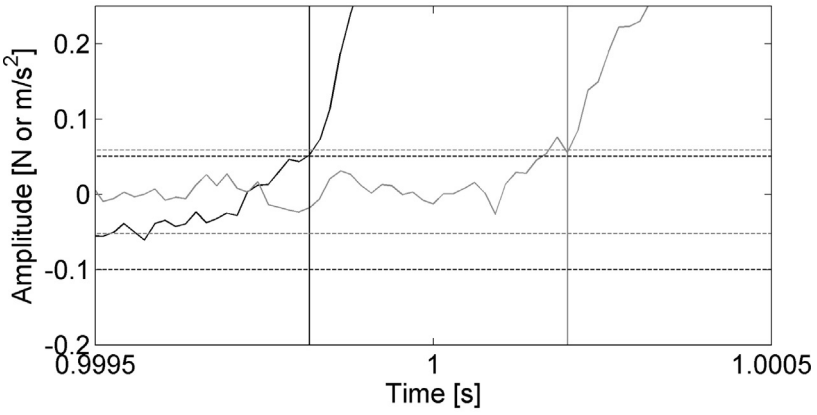

(b)

Fig. 5. (a) Example of hammer (dark grey solid line) and accelerometer (light grey solid line) signals from a sonic test. (b) Detail of figure (a) close to the impact time. Horizontal lines indicate the limits defined in Eq. (1) for the hammer (dark grey dashed lines) and the accelerometer (light grey dashed lines).

ultrasonic and sonic tests, respectively. As a result, a set of 10 and 30 values of the velocity, respectively, are obtained.

The quality and reliability of the obtained set of velocities are analyzed in terms of the scattering of their values. First, a criterion is established to define as outlier any result that differs more than a certain percentage (parameter Δ) of the median of the obtained set of velocities. The median is recalculated after the identified outliers are disregarded and the outlier criterion is applied again to the resulting set of results until a final set of samples with no outliers is obtained. In order to consider valid a resulting set of results, the number of identified outliers is limited to a certain number (parameter *NOutl*).

Since the values of the identified velocities depend on the values of the different parameters presented, an automated search of their optimal values is also done by the automated procedure. Results are obtained for the values of each parameter defined within a specific range defined by the user. The step (parameter *Step*) for the variation of each parameter during the search is also be selected by the user. The optimum set of values of the parameters is defined as that one with the lowest standard deviation of the obtained set of velocities. The average value of this set is considered as the most accurate measurement of the WPV.

3. Results and discussion

In accordance with the presented objectives of the paper, the most relevant results are presented next. Firstly, the finding of the most suitable parameters for the application of the automated procedure for signal identification is discussed and their values are presented. Secondly, the values of the WPV identified for all the specimens are analyzed and compared.

3.1. Values of the parameters for the automated WPV identification

In order to find the most suitable range for the parameters search, a sensitivity analysis of the results obtained for each parameter should be carried out in order to find a reasonable searching range for it. Due to the number of the parameters considered, the possible combinations between all of them dramatically increase when the range for each one is unnecessarily big and therefore the computational time may become a limitation in practice. This preliminary inspection of the results must be done by a simultaneous detailed visual check of the nature of the signals close to the time of interest (beginning of the impact for the excitation and arrival of the wave for the receiver), so the effect on the change of the value of each parameter can be understood. From visual inspection, values of each parameter can be identified as reasonable when approximate candidate samples are identified and no erroneous results are obtained.

When performing this task, it must be also taken into account that the parameters are not totally independent from each other. For instance, as parameter *NPt* increases, condition (3) can be easily fulfilled and therefore the requirement for the increasing or decreasing rate of the signal is less strict, unless the parameter

Table 3
Range of values defined for each parameter for the search of the optimal set.

–	$[\alpha_{exc}]$	$[\alpha_{rec}]$	[NPt]	[NRatio]	$[\beta_{exc}]$	$[\beta_{rec}]$	$[\Delta_{\%}]$	NOutl	[*Step*]
Sonic	[6,9]	[2,4]	[2,3]	[2,4]	1.4	1.05	15	20	1
Ultrasonic	–	2	[5,10]	–	–	–	15	6	1

NRatio is also increased accordingly. This increasing or decreasing trend is previously controlled by the effect of parameters α and β, which should be defined considering the oscillating nature and stability of the ambient noise.

On the other hand, the stability of the set of results is also affected by the selection of the values of parameters Δ and *NOutl*. The higher parameter Δ is, the less number of outliers are identified and therefore the limitation of the maximum number of outliers allowed (*NOutl*) is more easily accomplished. In addition, as *NOutl* increases and Δ decreases, the number of valid identified WPV becomes smaller and with less deviation between their values. As a consequence, the standard deviation of the resulting set of identified WPV is also smaller and the set of results can be erroneously considered more stable than it actually might be.

In this work, the range for each parameter that was found to be suitable for this work is defined in Table 3. In order to reduce the computational time, some of the parameters were fixed to a specific value after some manual inspection of its influence on the final results. In the case of the ultrasonic tests, a reduced number of parameters were used because of the higher signal-to-noise ratio of the signal and the absence of an excitation signal to be analyzed.

3.2. Evaluation of SWPV and UWPV

Figs. 6 and 7 show the identified SWPV and UWPV for each load step (Load 0, Load 1 and Load 2), for each specimen and for each measuring point. The corresponding values are listed in Tables 4–9. Some relevant phenomena can be identified. First, the velocities decrease as the level of supported load increase. Due to the internal damage (disaggregation, cracking, etc.) induced in the material by the applied load, the elastic waves find more resistance to propagate from one side of the specimen to the other. Second, due to

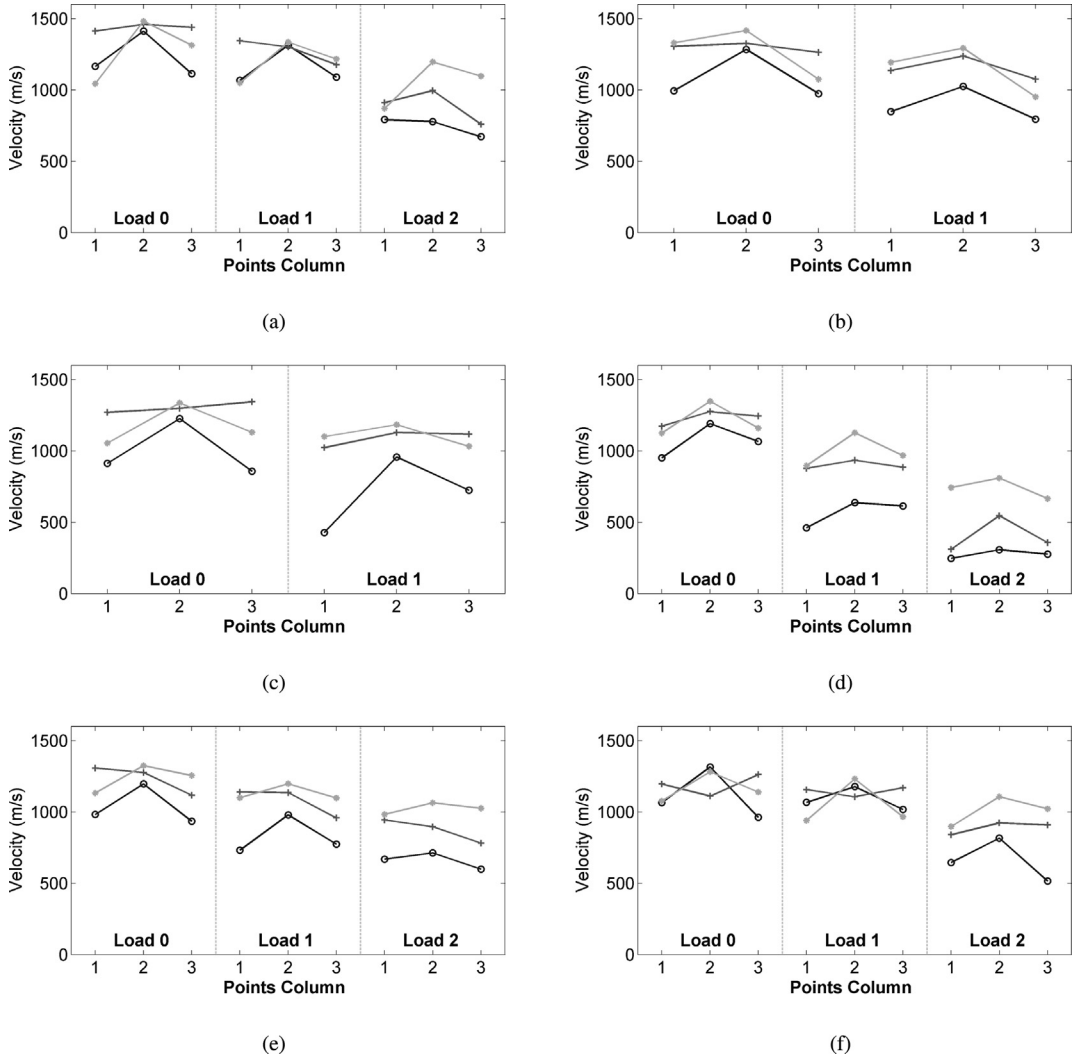

Fig. 6. SWPV at Load 0, Load 1 and Load 2, for each measuring point and for specimens (a) V1, (b) V2, (c) V3, (d) V4, (e) V5 y (f) V6. Dark (o), medium (+) and light (*) grey lines correspond to top, middle and bottom rows of measuring points.

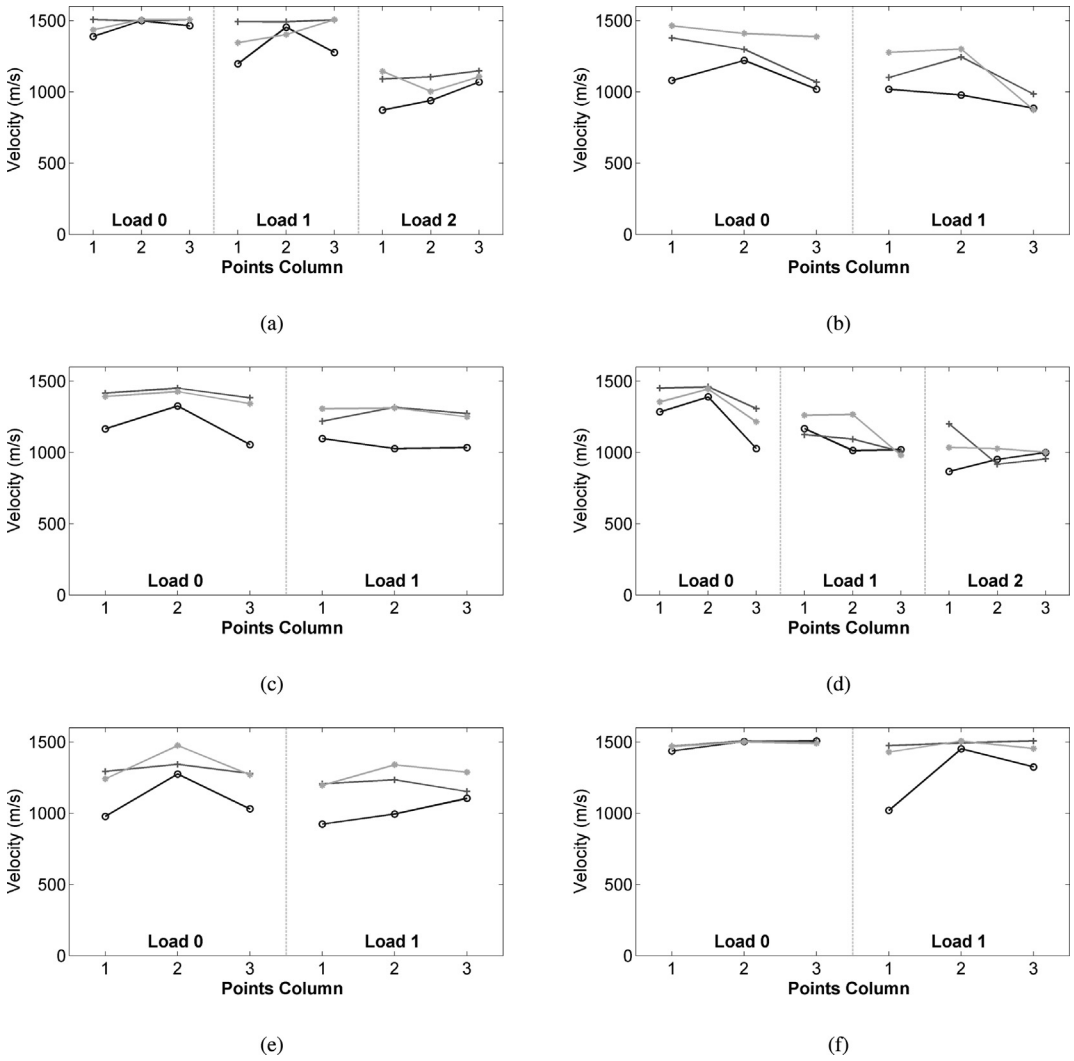

Fig. 7. UWPV at Load 0, Load 1 and Load 2, for each measuring point and for specimens (a) V1, (b) V2, (c) V3, (d) V4, (e) V5 y (f) V6. Dark (o), medium (+) and light (*) grey lines correspond to top, middle and bottom rows measuring points.

Table 4
Values of SWPV and UWPV obtained for each load level and measuring point for specimen V1.

	SWPV (m/s)			USWPV (m/s)		
Point	Load 0	Load 1	Load 2	Load 0	Load 1	Load 2
T1	1165.5	1068.0	792.5	1389.0	1197.3	872.8
T2	1411.8	1313.2	777.8	1499.3	1454.1	938.6
T3	1114.0	1089.2	671.7	1464.1	1276.7	1068.5
M1	1413.5	1343.8	910.8	1507.5	1492.4	1089.9
M2	1459.6	1301.6	995.2	1497.5	1491.6	1105.2
M3	1438.9	1176.3	759.6	1507.5	1505.7	1147.8
B1	1043.7	1049.3	870.2	1435.6	1345.1	1143.8
B2	1481.1	1335.1	1196.2	1507.5	1401.8	1002.6
B3	1313.6	1216.5	1097.0	1507.5	1506.4	1105.9

the compaction process, a gradient of the compaction level can be expected from the bottom to the upper part of the specimen. As a result, propagation velocities increase from top to bottom areas of the specimens. Moreover, since the compaction is more difficult to be efficiently applied in areas close to the corners of the mold, the compaction level may be lower at those zones. As a result, for each line of measuring points, the central points (labeled as '2') exhibit higher velocities than lateral points (labeled as '1' and '3'). In the work of Bernat-Maso et al. [18], higher UWPV were found for the upper part of rammed earth samples. However, in that work, a quasi-static compaction process of the whole specimen was applied for the manufacturing process. In such a case, a higher compaction level can be expected in the upper part of the sample, where particles have been moved and reorganized more significantly.

The previous observations clearly apply for the sonic test results. However, results for the ultrasonic tests are not clearly consistent in terms of the described gradients of velocities caused

Table 5
Values of SWPV and UWPV obtained for each load level and measuring point for specimen V2.

	SWPV (m/s)			USWPV (m/s)		
Point	Load 0	Load 1	Load 2	Load 0	Load 1	Load 2
- T1	994.5	848.1	–	1079.8	1017.8	–
T2	1283.7	1024.7	–	1220.6	978.0	–
T3	974.1	794.4	–	1018.6	884.3	–
M1	1305.3	1135.1	–	1377.9	1100.7	–
M2	1326.8	1237.5	–	1298.1	1245.3	–
M3	1263.5	1075.6	–	1068.0	984.4	–
B1	1330.1	1192.3	–	1463.5	1276.8	–
B2	1416.3	1292.9	–	1410.7	1300.3	–
B3	1074.4	951.0	–	1386.7	873.4	–

Table 6
Values of SWPV and UWPV obtained for each load level and measuring point for specimen V3.

	SWPV (m/s)			USWPV (m/s)		
Point	Load 0	Load 1	Load 2	Load 0	Load 1	Load 2
T1	912.1	427.5	–	1166.1	1097.5	–
T2	1225.5	957.5	–	1326.8	1027.9	–
T3	856.8	724.0	–	1055.2	1034.2	–
M1	1269.8	1022.8	–	1416.4	1219.6	–
M2	1298.8	1128.9	–	1450.6	1316.8	–
M3	1344.0	1118.2	–	1383.9	1272.5	–
B1	1054.5	1100.7	–	1392.5	1306.7	–
B2	1336.2	1183.8	–	1427.1	1312.3	–
B3	1129.6	1032.0	–	1343.2	1250.2	–

Table 7
Values of SWPV and UWPV obtained for each load level and measuring point for specimen V4.

	SWPV (m/s)			USWPV (m/s)		
Point	Load 0	Load 1	Load 2	Load 0	Load 1	Load 2
T1	951.7	460.8	247.1	1284.5	1167.0	867.1
T2	1190.6	637.3	306.4	1390.2	1013.6	951.3
T3	1066.5	614.4	275.9	1027.4	1018.8	999.8
M1	1173.3	877.6	310.1	1450.8	1125.1	1200.1
M2	1276.0	934.5	545.9	1460.6	1093.7	918.1
M3	1244.1	885.3	357.0	1307.6	1007.7	954.7
B1	1125.2	896.5	742.4	1355.3	1261.2	1035.0
B2	1347.6	1127.4	809.4	1445.0	1266.3	1027.3
B3	1160.1	967.1	665.2	1216.1	981.6	1001.8

Table 8
Values of SWPV and UWPV obtained for each load level and measuring point for specimen V5.

	SWPV (m/s)			USWPV (m/s)		
Point	Load 0	Load 1	Load 2	Load 0	Load 1	Load 2
T1	982.2	732.2	669.6	977.6	923.4	–
T2	1195.9	979.9	712.3	1275.1	994.3	–
T3	935.2	773.9	598.2	1029.8	1104.0	–
M1	1308.2	1139.7	943.3	1293.4	1206.1	–
M2	1276.7	1135.4	896.0	1342.8	1233.9	–
M3	1117.3	957.9	781.0	1278.2	1152.4	–
B1	1132.7	1099.2	982.7	1241.0	1194.9	–
B2	1324.5	1198.0	1064.4	1474.6	1340.0	–
B3	1255.4	1098.0	1025.9	1269.3	1287.9	–

by a non–homogeneous compaction process nor the damage level. Moreover, the uncertainty in the identification of ultrasonic velocities increases as the material is more damaged because of the scattering and attenuation of the elastic waves. As a result, for instance, no results could be obtained for Load 2 for specimens V5 and V6, whereas sonic velocities could be well determined. Another relevant result is that values of UWPV are higher than SWPV.

In order to compare the relative uncertainty from both sonic and ultrasonic velocities, Fig. 8 shows a statistical analysis of the results for all the specimens at each measuring point for the undamaged situation (Load 0). The median, the 25% and 75% percentiles and the extreme values of each set of results are represented. It can be seen that the scattering of the results is significantly lower for the sonic tests. Moreover, the aforementioned effect of the compaction gradient can be observed for the SWPV but it is not clear for UWPV.

In order to better illustrate the effect of the decrease of the wave propagation velocities as the applied load increase, Fig. 9

Table 9
Values of SWPV and UWPV obtained for each load level and measuring point for specimen V6.

	SWPV (m/s)			USWPV (m/s)		
Point	Load 0	Load 1	Load 2	Load 0	Load 1	Load 2
T1	1065.9	1066.9	645.8	1436.3	1019.4	–
T2	1315.4	1177.9	816.3	1502.4	1452.0	–
T3	962.3	1017.5	515.4	1507.5	1324.6	–
M1	1196.0	1156.5	840.1	1470.8	1473.7	–
M2	1111.4	1106.1	923.5	1507.5	1493.8	–
M3	1262.5	1169.2	909.3	1497.0	1507.5	–
B1	1077.4	939.6	897.4	1467.7	1429.1	–
B2	1280.9	1232.0	1106.6	1500.5	1506.0	–
B3	1138.9	965.8	1021.6	1490.1	1453.3	–

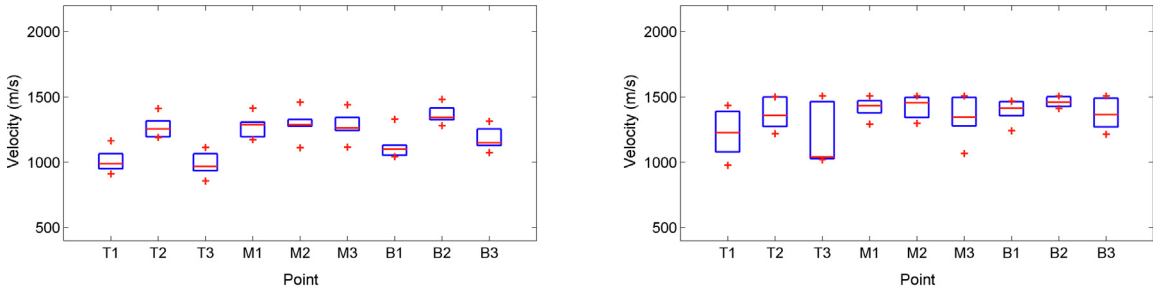

Fig. 8. Statistical analysis of (a) SWPV and (b) UWPV at each measuring point for all specimens. The red line indicates the median of the results at each point, the box indicates the 25% and 75% percentiles and the markers indicate the most extreme values.

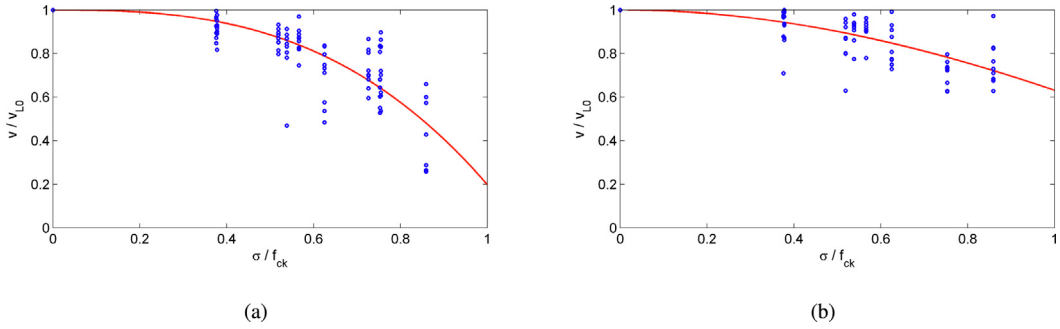

Fig. 9. Normalized wave propagation velocities (v/V_{L0}) for the corresponding normalized applied load (σ/f_c) for (a) sonic and (b) ultrasonic tests.

shows the relationship between the values of the obtained velocities at loading levels L1 and L2, normalized with their corresponding values at Load 0, and the normalized stress values for each load with the compressive strength (f_c) of each specimen. A third order polynomial fit of the data is included in Fig. 9. It illustrates that, as the level of relative load increases, the decrease in the wave propagation velocities becomes more significant. It can be observed that the trend is more clear for the sonic tests, being more sensitive to the presence of damage due to the applied load.

For comparison purpose, some reference values of wave propagation velocities that can be found in the literature are summarized in Table 10. A broad range of values can be found in the literature for rammed earth or other traditional building materials (adobe, stone, granite). The specific characteristics of each material (composition, age, conservation state, manufacturing process, etc), can affect the results. However, despite the scattering of the results, it can be seen that rammed earth can exhibit similar values than other clay or stone based building materials. A typical range can be roughly defined between 1000 m/s and 2500 m/s. The values obtained in the present work are in agreement with previous results from other authors.

The scattering of results of UWPV and SWPV for rammed earth walls can be explained because of different soil properties, manufacturing process, age, etc. However, in this paper, even using the same material and controlled manufacturing conditions, different velocities can be observed for different specimens. This result does not invalidate the application of the sonic and ultrasonic tests for the inspection of rammed earth constructions, but indicates that the identified velocities should not be considered by themselves in an absolute way for the evaluation of the construction properties or the conservation state. They should be considered with caution by comparing them with some reference values. The potential use of the sonic and ultrasonic tests relies mainly on a qualitative analysis of the velocities identified at different points of the same construction, as it has been shown in the paper. In addition, the monitoring of the WPV along time is necessary to obtain reference values to compare with.

Table 10
Reference values of SWPV and UWPV from the literature.

Velocity [m/s]	SWPV	UWPV	Material	Reference
≃ [1300, 1700]	–	X	Rammed Earth	[14]
≃ [1400, 1500]	–	X	Rammed Earth	[18]
≃ 2000	–	X	Rammed Earth	[15]
≃ [500,600]	X	–	Rammed Earth	[24]
≃ 500	X	–	Rammed Earth (historical)	[25]
≃ [2000,2500]	X	–	Rammed Earth	[22,23]
≃ 1600	–	X	Adobes	[19]
≃ [200,900]	X	–	Stone Masonry	[48]
≃ [2500,3000]	X	–	Stone Masonry	[21]
≃ [1000, 1500]	–	X	Granite Masonry	[49]
≃ 4000	X	–	Concrete	[50]

4. Conclusions

The presented results show that the identification of SWPV and UWPV can be considered valid tools for quality control and inspection of rammed earth constructions. Areas where the propagation velocities are lower can indicate the presence of a higher level of damage or lower compaction. The practical efficiency of the tests is enhanced by the application of an automated algorithm for the determination of the time-of-flight of the elastic waves. This automated procedure avoids the time consuming and subjective task of visual inspection of the recorded signals. Data from a large number of tests and number of measuring points can be efficiently processed. From the present research, some reference values of the parameters involved in the proposed algorithm have been presented so they can lead to greater efficiency in the management of the experimental data and to improve the quality and reliability of the results from future experimental campaigns. The presented procedure is easy to be implemented and tailored by any technician to be used in practice.

The results also show that higher consistency and lower uncertainty are found for SWPV than for UWPV. Moreover, SWPV is more sensitive to changes in the material properties due to different compaction levels or to the presence of damage. On the other hand, because of the high frequency of the ultrasonic waves and the resultant scattering of elastic waves in the presence of damage, the UWPV can not be determined for levels of global damage for which the SWPV can be obtained. For these reasons, sonic tests are considered more powerful and robust than ultrasonic tests. However, conclusions drawn from the present analysis can be considered as preliminary. Further research is required on the analysis and comparative study of the performance and limitations of both inspection techniques. The influence of different specimen geometries (specially the distance between source and receiver), soil properties, stabilizers, etc. should be considered.

The paper shows that different values of WPV can be determined for samples of the same material and that have been manufactured following the same procedure and under controlled conditions. More significant differences are found between previously obtained values for rammed earth samples from different authors. Thus, the values of the identified WPV for a specific specimen should not be considered by themselves as valid quality control parameters in an absolute way. A reliable analysis about its conservation state should be done from the relative distribution of WPV at different points of the specimen. Monitoring these values along time can also provide valid information for the analysis of the evolution of the conservation state.

As future work, the authors propose the evaluation of WPV along different directions and the application of a compressive load perpendicular to the compaction direction in order to assess the anisotropy of the material. On the other hand, mechanical properties along both directions (static and dynamic Young modulus, compressive strength) should be determined and analyzed. The influence of moisture content on UWPV and SWPV is also an interesting issue to be addressed.

CRediT authorship contribution statement

J.D. Rodríguez-Mariscal: Conceptualization, Methodology, Software, Writing - original draft, Writing - review & editing. **J. Canivell:** Conceptualization, Methodology, Supervision, Writing - original draft, Writing - review & editing. **M. Solís:** Conceptualization, Methodology, Software, Funding acquisition, Supervision, Writing - original draft, Writing - review & editing.

Declaration of Competing Interest

The authors declare that they have no known competing financial interests or personal relationships that could have appeared to influence the work reported in this paper.

Acknowledgements

This work was supported by Junta de Andalucia (Consejería de Economía y Conocimiento) through research project US-126491 and the Spanish Ministry of Science, Innovation and Universities (Ministerio de Ciencia, Innovación y Universidades) through research project PID2019-109622RB-C21.

References

[1] H. Schroeder, Sustainable Building with Earth, Springer (2016), https://doi.org/10.1007/978-3-319-19491-2.
[2] J. Cid, F.R. Mazarrón, I. Caóas, Las normativas de construcción con tierra en el mundo, Informes de la Construcción 523 (2011) 159–169, https://doi.org/10.3989/ic.10.011.
[3] M.I. Gomes, T.D. Gonçalves, P. Faria, Unstabilized Rammed earth: characterization of material collected from old constructions in South Portugal and comparison to normative requirements, Int. J. Architectural Heritage 8 (2) (2014) 185–212, https://doi.org/10.1080/15583058.2012.683133.
[4] H. Niroumand, J.A. Barcelo, C.J. Kibert, M. Saaly, Evaluation of Earth Building Tools in Construction (EBTC) in earth architecture and earth buildings, Renew. Sustain. Energy Rev. 70 (Supplement C) (2017) 861–866, https://doi.org/10.1016/j.rser.2016.11.267. URL: http://www.sciencedirect.com/science/article/pii/S1364032116310486.
[5] J.D. Rodríguez-Mariscal, M. Solís, H. Cifuentes, Methodological issues for the mechanical characterization of unfired earth bricks, Constr. Build. Mater. 175 (2018) 804–814, https://doi.org/10.1016/j.conbuildmat.2018.04.118.
[6] J. Canivell, J.J. Martín-del Río, R.M. Falcón, C. Rubio-Bellido, Rammed Earth Construction: A Proposal for a Statistical Quality Control in the Execution Process, Sustainability 12(7) (2020) 2830. doi:10.3390/su12072830. https://www.mdpi.com/2071-1050/12/7/2830..
[7] C. Mileto, F. Vegas López-Manzanares, L. Villacampa Crespo, L. García-Soriano, The Influence of Geographical Factors in Traditional Earthen Architecture: The Case of the Iberian Peninsula, Sustainability 11(8) (2019) 2369. doi:10.3390/su11082369. https://www.mdpi.com/2071-1050/11/8/2369..
[8] S. Samadianfard, V. Toufigh, Energy use and thermal performance of rammed-earth materials, J. Mater. Civ. Eng. 32 (10) (2020) 04020276, https://doi.org/10.1061/(ASCE)MT.1943-5533.0003364.
[9] V. Toufigh, E. Kianfar, The effects of stabilizers on the thermal and the mechanical properties of rammed earth at various humidities and their

environmental impacts, Constr. Build. Mater. 200 (2019) 616–629, https://doi.org/10.1016/j.conbuildmat.2018.12.050. URL: https://www.sciencedirect.com/science/article/pii/S0950061818330319.
[10] I. Lombillo, L. Villegas, E. Fodde, C. Thomas, In situ mechanical investigation of rammed earth: calibration of minor destructive testing, Constr. Build. Mater. 51 (2014) 451–460, https://doi.org/10.1016/J.CONBUILDMAT.2013.10.090. URL: http://www.sciencedirect.com/science/article/pii/S0950061813010118?via%3Dihub#b0165.
[11] Q.B. Bui, Assessing the rebound hammer test for rammed earth material, Sustainability (Switzerland) 9 (10) (2017) 11–17, https://doi.org/10.3390/su9101904.
[12] B. González-Sánchez, A. Navarro Ezquerra, L. Rincon, Correlación de NDT versus resistencia a compresión en tapia, Congrès mondial sur les architectures de terra (2016) 106..
[13] Q.B. Bui, J.C. Morel, S. Hans, N. Meunier, Compression behaviour of non-industrial materials in civil engineering by three scale experiments: the case of rammed earth, Mater. Struct./Materiaux et Constructions 42 (8) (2009) 1101–1116, https://doi.org/10.1617/s11527-008-9446-y.
[14] J. Canivell, J.J. Martin-del Rio, F. Alejandre, J. García-Heras, A. Jimenez-Aguilar, Considerations on the physical and mechanical properties of lime-stabilized rammed earth walls and their evaluation by ultrasonic pulse velocity testing, Constr. Build. Mater. 191 (2018) 826–836, https://doi.org/10.1016/J.CONBUILDMAT.2018.09.207. URL: https://www.sciencedirect.com/science/article/pii/S0950061818323961#fn1.
[15] J.J. Martín-del Rio, J. Canivell, R.M. Falcón, The use of non-destructive testing to evaluate the compressive strength of a lime-stabilised rammed-earth wall: Rebound index and ultrasonic pulse velocity, Constr. Build. Mater. 242. doi:10.1016/j.conbuildmat.2020.118060..
[16] UNE-AENOR, UNE-EN 12504-4 Testing Concrete. Part 4: Determination of Ultrasonic Pulse Velocity, Asociación Española de Normalización y Certificación, Madrid, Spain, 2007..
[17] P. Gerard, M. Mahdad, A. Robert McCormack, B. François, A unified failure criterion for unstabilized rammed earth materials upon varying relative humidity conditions, Constr. Build. Mater. doi:10.1016/j.conbuildmat.2015.07.100..
[18] E. Bernat-Maso, E. Teneva, C. Escrig, L. Gil, Ultrasound transmission method to assess raw earthen materials, Constr. Build. Mater. 156 (2017) 555–564, https://doi.org/10.1016/J.CONBUILDMAT.2017.09.012. URL: https://www.sciencedirect.com/science/article/pii/S0950061817318032?via%3Dihub.
[19] R. Aguilar, M. Montesinos, S. Uceda, Mechanical characterization of the structural components of Pre-Columbian earthen monuments: analysis of bricks and mortar from Huaca de la Luna in Perú, Case Stud. Constr. Mater. 6 (2017) 16–28, https://doi.org/10.1016/j.cscm.2016.11.003.
[20] L. Binda, A. Saisi, C. Tiraboschi, Application of sonic tests to the diagnosis of damaged and repaired structures, NDT & E Int. 34 (2) (2001) 123–138, https://doi.org/10.1016/S0963-8695(00)00037-2. URL: https://www.sciencedirect.com/science/article/pii/S0963869500000372.
[21] L.F. Miranda, J. Rio, J. Miranda Guedes, A. Costa, Sonic Impact Method – a new technique for characterization of stone masonry walls, Constr. Build. Mater. 36 (2012) 27–35, https://doi.org/10.1016/j.conbuildmat.2012.04.018.
[22] R.A. Silva, O. Domínguez-Martínez, D.V. Oliveira, E.B. Pereira, Comparison of the performance of hydraulic lime- and clay-based grouts in the repair of rammed earth, Constr. Build. Mater. 193 (2018) 384–394, https://doi.org/10.1016/J.CONBUILDMAT.2018.10.207. URL: https://www.sciencedirect.com/science/article/pii/S0950061818326242#s0040.
[23] O. Dominguez-Martínez, Preservation and repair of rammed earth constructions., Structural Analysis of Monuments and Historical Constructions Master Thesis (September) (2015) 1–103. doi:10.13140/RG.2.1.2202.9282.http://www.msc-sahc.org/upload/docs/new.docs/2015_OGonzalez.pdf..
[24] R.A. Silva, N. Mendes, D.V. Oliveira, A. Romanazzi, O. Domínguez-Martínez, T. Miranda, Evaluating the seismic behaviour of rammed earth buildings from Portugal: From simple tools to advanced approaches, Eng. Struct. 157 (2018) 144–156, https://doi.org/10.1016/J.ENGSTRUCT.2017.12.021. URL: https://www.sciencedirect.com/science/article/pii/S0141029617321375?via%3Dihub#b0040.
[25] M. Giamello, F. Fratini, S. Mugnaini, E. Pecchioni, F. Droghini, F. Gabbrielli, E. Giorgi, E. Manzoni, F. Casarin, A. Magrini, F. Randazzo, Earth masonries in the medieval Grange of cuna - siena (Italy), J. Mater. Environ. Sci. 7 (10) (2016) 3509–3521.
[26] UNE-AENOR, UNE-EN ISO 17892–4. Geotechnical investigation and testing - Laboratory testing of soil - Part 4: Determination of particle size distribution., Asociación Española de Normalización y Certificación, Madrid, Spain..
[27] AENOR, UNE 103103:1994. Determination of the liquid limit of a soil by the Casagrande apparatus method, Asociación Española de Normalización y Certificación, Madrid, Spain, 1994..
[28] AENOR, UNE 103104:1993. Test for plastic limit of a soil, Asociación Española de Normalización y Certificación, Madrid, Spain, 1993..
[29] S. Kenai, R. Bahar, M. Benazzoug, Experimental analysis of the effect of some compaction methods on mechanical properties and durability of cement stabilized soil, J. Mater. Sci. 41 (21) (2006) 6956–6964, https://doi.org/10.1007/s10853-006-0226-1.
[30] D.D. Tripura, K.D. Singh, Characteristic properties of cement-stabilized rammed earth blocks, J. Mater. Civ. Eng. 27 (7) (2015) 04014214, https://doi.org/10.1061/(ASCE)MT.1943-5533.0001170.
[31] L. Xu, H. Wong, A. Fabbri, F. Champiré, D. Branque, A unified compaction curve for raw earth material based on both static and dynamic compaction tests, Mater. Struct. 54 (1) (2021) 5, https://doi.org/10.1617/s11527-020-01595-5.
[32] Q.-B. Bui, J.-C. Morel, S. Hans, P. Walker, Effect of moisture content on the mechanical characteristics of rammed earth, Constr. Build. Mater. 54 (2014) 163–169, https://doi.org/10.1016/j.conbuildmat.2013.12.067.
[33] ASTM, ASTM D698 - 12e2. Standard Test Methods for Laboratory Compaction Characteristics of Soil Using Standard Effort, ASTM International, West Conshohocken, Penn., United States, 2012..
[34] AENOR, UNE 103500:1994. Geotecnia. Ensayo de compactación. Proctor normal, Asociación Española de Normalización y Certificación, Madrid, Spain, 1994.
[35] ASTM, ASTM D1557 - 12e1. Standard Test Methods for Laboratory Compaction Characteristics of Soil Using Modified Effort, ASTM International, West Conshohocken, Penn., United States, 2012..
[36] AENOR, UNE 103501:1994. Geotecnia. Ensayo de compactación. Proctor modificado, Asociación Española de Normalización y Certificación, Madrid, Spain, 1994..
[37] J.-J. Wang, Y. Yang, H.-P. Zhang, Effects of particle size distribution on compaction behavior and particle crushing of a mudstone particle mixture, Geotech. Geol. Eng. 32 (4) (2014) 1159–1164, https://doi.org/10.1007/s10706-014-9782-3.
[38] A. Koutous, E. Hilali, Case Studies in Construction Materials 11 (2019) e00303. doi:10.1016/J.CSCM.2019.E00303. https://www.sciencedirect.com/science/article/pii/S221450951930405X?via..
[39] V. Maniatidis, P. Walker, Structural capacity of rammed earth in compression, J. Mater. Civ. Eng. 20 (3) (2008) 230–238, https://doi.org/10.1061/(ASCE)0899-1561(2008)20:3(230).
[40] M. Hall, Y. Djerbib, Rammed earth sample production: context, recommendations and consistency, Constr. Build. Mater. 18 (4) (2004) 281–286, https://doi.org/10.1016/j.conbuildmat.2003.11.001.
[41] L. Miccoli, D.V. Oliveira, R.A. Silva, U. Müller, L. Schueremans, Static behaviour of rammed earth: experimental testing and finite element modelling, Mater. Struct. 48 (10) (2015) 3443–3456, https://doi.org/10.1617/s11527-014-0411-7.
[42] UNE-AENOR, UNE-EN-ISO-17892-1-2015 Geotechnical investigation and testing. Laboratory testing of soils. Part 1: Determination of water content., Asociación Española de Normalización y Certificación, Madrid, Spain, 2015..
[43] V. Maniatidis, P. Walker, A review of rammed earth construction, Developing rammed earth for UK housing (May) (2003) 109.http://staff.bath.ac.uk/abspw/rammedearth/review.pdf..
[44] UNE-AENOR, UNE-EN 1936:2007 Natural stone test methods - Determination of real density and apparent density, and of total and open porosity, Asociación Española de Normalización y Certificación, Madrid, Spain, 2007..
[45] H. Houben, H. Guillaud, CRAterre., Intermediate Technology Publications., Earth construction: a comprehensive guide, Intermediate Technology Publications, 1994..
[46] M.R. Valluzzi, E. Cescatti, G. Cardani, L. Cantini, L. Zanzi, C. Colla, F. Casarin, Calibration of sonic pulse velocity tests for detection of variable conditions in masonry walls, Constr. Build. Mater. 192 (2018) 272–286, https://doi.org/10.1016/J.CONBUILDMAT.2018.10.073. URL: https://www.sciencedirect.com/science/article/pii/S0950061818324346.
[47] E. Cescatti, L. Rosato, M. Valluzzi, F. Casarin, An Automatic Algorithm for the Execution and Elaboration of Sonic Pulse Velocity Tests in Direct and Tomographic Arrangements, Rilem doi:10.1007/978-3-319-99441-3..
[48] R. Martini, J. Carvalho, N. Barraca, A. Arêde, H. Varum, Advances on the use of non-destructive techniques for mechanical characterization of stone masonry: GPR and sonic tests, Proc. Struct. Integr. 5 (2017) 1108–1115, https://doi.org/10.1016/j.prostr.2017.07.096.
[49] E. Manning, L.F. Ramos, F.M. Fernandes, Direct Sonic and Ultrasonic Wave Velocity in Masonry under Compressive Stress, in: IMC (Ed.), 9th International Masonry Conference, Guimaraes (Portugal), 2014. URL: https://repositorium.sdum.uminho.pt/bitstream/1822/30864/1/ID14219IMC-Paper-Manning.pdf..
[50] L. Qixian, J.H. Bungey, Using compression wave ultrasonic transducers to measure the velocity of surface waves and hence determine dynamic modulus of elasticity for concrete, Constr. Build. Mater. 10 (4) (1996) 237–242, https://doi.org/10.1016/0950-0618(96)00003-7.